

# Indirect and monojet constraints on scalar leptoquarks

Alexandre Alves,<sup>1,\*</sup> Oscar J. P. Éboli,<sup>2,†</sup> Giovanni Grilli di Cortona,<sup>2,3,‡</sup> and Roberto R. Moreira<sup>2,§</sup>

<sup>1</sup>*Departamento de Física, Universidade Federal de São Paulo, UNIFESP, Diadema, São Paulo, Brazil*

<sup>2</sup>*Instituto de Física, Universidade de São Paulo, São Paulo, Brazil*

<sup>3</sup>*Institute of Theoretical Physics, Faculty of Physics,  
University of Warsaw, ul. Pasteura 5, PL-02-093 Warsaw, Poland*

We obtain constraints on first- and second-generation scalar leptoquarks using the available data on dilepton (Drell-Yan) and monojet searches at the CERN Large Hadron Collider. Assuming that the leptoquark interactions respect the Standard Model gauge symmetries as well as lepton and baryon numbers, we show that the study of dilepton production enlarges the exclusion region on the mass and coupling plane with respect to the pair production searches for first-generation leptoquarks. Moreover, the monojet channel leads to a larger excluded parameter region for moderate to large values of the leptoquark Yukawa coupling than the presently available experimental results.

## I. INTRODUCTION

The CERN Large Hadron Collider (LHC) has gathered a large amount of data that has been used not only to probe the Standard Model (SM), but also to look for new physics. The SM does not have any state that couples to lepton-quark pairs, therefore, the discovery of such a state would be an indubitable sign of Physics beyond the SM. In fact this is an ongoing search by the LHC collaborations; see, for instance, Refs. [1, 2].

Leptoquarks are particles which interact with quark-lepton pairs. They appear in a plethora of models where quarks and leptons are treated in the same footing. The first appearance of leptoquarks was in the Pati-Salam model [3, 4] and they are also present in Grand Unified Theories [5], composite models [6], or in supersymmetric models with violation of  $R$  parity [7]. Leptoquarks modify the low-energy physics which, in turn, leads to constraints on their masses and couplings. For instance, leptoquarks might contribute to the decay of mesons [8], induce flavor changing neutral currents (FCNC) [4, 8], give rise to lepton flavor violating decays [9], and contribute to the radiative correction to  $Z$  physics [10, 11]. Recently some anomalies were observed that point towards lepton flavor universality violation in neutral- and charged-current processes [12–21]. One possible explanation to the departures from the SM is the existence of leptoquarks with masses  $\mathcal{O}(\text{TeV})$ ; see, for instance, Refs. [22–26] and references therein.

Since leptoquarks carry color, they can be pair produced via QCD [27] at the LHC and the main advantage of this channel is that the production cross section depends only on the leptoquark mass. Presently most of the LHC searches for leptoquarks are based on their pair production. The LHC RUN 1 data excludes first- (second-) generation scalar leptoquarks with masses smaller than 1050 (1080) GeV [28, 29] provided the leptoquark decays exclusive into a charged lepton and a jet. The already available results from LHC RUN 2 expands these limits to 1435 GeV and 1520 GeV for first- and second-generation leptoquarks, respectively [2, 30].

Leptoquarks can also be produced singly in association with a lepton through its coupling to a quark-lepton pair [31, 32]. In fact, this process has a larger phase space than the leptoquark pair production and for  $\mathcal{O}(1)$  couplings and 100% branching ratio into charged lepton plus up quark, the bounds ( $\mathcal{O}(1.3\text{--}1.7)$  TeV) from the Run I data of the LHC can be even stronger than the pair production ones [33]. At the LHC it is also possible to look for indirect signs of leptoquarks in the production of charged lepton pairs [31, 32].

---

\*Electronic address: aalves.unifesp@gmail.com

†Electronic address: eboli@if.usp.br

‡Electronic address: ggrillidc@fuw.edu.pl

§Electronic address: robertor@fma.if.usp.br

Leptoquarks coupling to a neutrino and a quark give rise to monojet events due to their single production. In this case, the leptoquark decay leads to a hard missing transverse energy spectrum peaking around half the leptoquark mass. It is interesting to notice that models where leptoquarks couple to dark matter [34] with sizable branching ratios could also be constrained by these monojet searches. At the same time they alleviate other constraints due to the diminished leptoquark branching ratio to SM lepton plus quark. Moreover, the LHC collaborations also searched for leptoquarks in the mono-bottom [35–37] and mono-top quark [38, 39] channels which have been explored in the search for dark matter. These channels constitute alternatives to pair production in the case where the third-generation leptoquarks are too heavy.

If leptoquarks are too heavy to be pair produced at the LHC, single production and indirect effects in lepton pair production remain as alternatives to search for these particles [31]. In this work we study the attainable bounds on first- and second-generation scalar leptoquarks using the available data on lepton pair production and the monojet searches for dark matter [40]. Our results depend on the leptoquark mass as well as its Yukawa coupling to quark-lepton pairs. As a consequence, they will yield more information on the leptoquark properties if a signal is observed, complementing the leptoquark pair production searches. We show that the study of dilepton production enlarges the exclusion region in the plane mass and coupling with respect to the pair production searches. Additionally, the monojet channel for first-generation leptoquarks also leads to a larger exclusion region than the canonical  $\ell^+\ell^-jj$  and  $\ell^\pm\nu jj$  (with  $\ell = e$  and  $\mu$ ) topologies for moderate and large values of the leptoquark Yukawa coupling. The monojet channel is also able to probe a larger fraction of the parameter space than the  $jjE_T^{\text{miss}}$  final state [41].

## II. ANALYSES FRAMEWORK

In order to describe the leptoquark interactions at the presently available energies we assume that leptoquarks are the only accessible states from an extension of the SM. Moreover, we impose that their interactions respect the SM gauge symmetry  $SU(3)_c \otimes SU(2)_L \otimes U(1)_Y$ . Furthermore, due to the stringent bounds coming from proton lifetime experiments the leptoquark interactions are required to respect baryon and lepton numbers. Within these hypotheses, there are five distinct possibilities for scalar leptoquarks [42]: two  $SU(2)_L$  singlet states ( $S_1$  and  $\tilde{S}_1$ ), two doublet states ( $R_2$  and  $\tilde{R}_2$ ) and one triplet ( $S_3$ ), whose interactions with quarks and leptons are

$$\begin{aligned} \mathcal{L}_{\text{eff}} = & (g_{1L} \bar{q}_L^c i\tau_2 \ell_L + g_{1R} \bar{u}_R^c e_R) S_1 + \tilde{g}_{1R} \bar{d}_R^c e_R \tilde{S}_1 + g_{3L} \bar{q}_L^c i\tau_2 \vec{\tau} \ell_L \cdot \vec{S}_3, \\ & + h_{2L} R_2^T \bar{u}_R i\tau_2 \ell_L + h_{2R} \bar{q}_L e_R R_2 + \tilde{h}_{2L} \tilde{R}_2^T \bar{d}_R i\tau_2 \ell_L, \end{aligned} \quad (2.1)$$

where  $q_L$  ( $\ell_L$ ) stands for the left-handed quark (lepton) doublet,  $u_R$ ,  $d_R$ , and  $e_R$  are the singlet components of the fermions,  $\tau_i$  are the Pauli matrices, and we denote the charge conjugated fermion fields by  $\psi^c = C\bar{\psi}^T$ . Moreover, we omit the flavor indices of the fermions. The couplings of the leptoquarks to the electroweak gauge bosons is determined by the  $SU(3)_c \otimes SU(2)_L \otimes U(1)_Y$  gauge invariance.

At low energies, leptoquarks give rise to flavor changing neutral current (FCNC) processes [4, 8, 43] that are very constrained. In order to avoid stringent bounds, we assume that the scalar leptoquarks couple only to a single generation of quarks and just one of leptons. In fact, we consider that the leptoquarks interact with the same generation of quarks and leptons. Notwithstanding, there is a residual amount of FCNC due to the mixing in the quark sector that leads to bounds on leptoquark couplings to the first two generations [44, 45]. Moreover, data on decays of pseudo-scalar mesons, like the pions, put stringent bounds on leptoquarks unless their couplings are chiral - that is, they are either left- or right-handed [8, 44, 45]. As a rule of a thumb, the low-energy data constrain first-generation-leptoquark masses to be larger than 0.5–1.0 TeV for leptoquark Yukawa couplings of the order of the proton charge  $e$  [46].

In our analysis we focus on leptoquarks that conserve fermion number  $F = 3B + L$ , *i.e.* the states  $R_2$  and  $\tilde{R}_2$ . For the sake of simplicity, we assume that leptoquarks belonging to a given  $SU(2)_L$  multiplet are degenerate. We study the following scenarios that satisfy the described low-energy bounds:

1.  $\tilde{R}_2$  coupling only to the first generation, *i.e.* only to down quarks, electrons and its neutrino. We label this scenario as  $\tilde{R}_2^d$ .
2.  $R_2$  coupled to the first generation and exhibiting only left-handed interactions ( $h_{2R} = 0$ ). In this case the leptoquarks interact with up quarks, electrons and the respective neutrino. We refer to this scenario as  $R_2^L$ .
3.  $\tilde{R}_2$  coupling only to the second generation – that is to strange quarks, muons and the corresponding neutrinos. We call this scenario  $\tilde{R}_2^s$ .

These scenarios allows us to obtain bounds on other leptoquarks. For instance, the constraints on  $R_2$  (second scenario) originating from the dilepton data can be easily translated into bounds on the singlet  $S_1$  or the third component of the triplet  $\tilde{S}_3$ . On the other hand, the dileptons limits in the first scenario can be readily transposed to  $\tilde{S}_1$  and one component of  $\tilde{S}_3$ . Furthermore, the  $\tilde{R}_2^s$  case is the one leading to the strongest constraints on second-generation leptoquarks.

In order to study leptoquarks at the LHC we consider their indirect effects in Drell-Yan processes [31]

$$pp \rightarrow e^+e^-/\mu^+\mu^- + X \quad (2.2)$$

as well as in monojet searches

$$pp \rightarrow j + E_T^{\text{miss}} \quad (2.3)$$

In the Drell-Yan 8 TeV analyses we use the data in Ref. [47] that contain the  $e^+e^-$  and  $\mu^+\mu^-$  invariant mass distribution in the fiducial region defined by the leading (subleading) lepton having  $p_T^\ell > 40$  GeV (30 GeV) and both leptons within the rapidity range  $|\eta| < 2.5$ . These results are given at QED Born level which simplifies the comparison with the leptoquark predictions. Since the 13 TeV Drell-Yan analyses have not been released by ATLAS and CMS we use the data on searches for new resonances decaying into lepton pairs given in Refs. [48, 49]. More specifically, the data used was<sup>1</sup>

Channel	kinematical range	# bins	Int. Lum.	Data set
$e^+e^-$	$116 < m_{ee} < 1500$ GeV	12	20.3 fb <sup>-1</sup>	ATLAS 8 TeV [47] Table 6
$\mu^+\mu^-$	$116 < m_{\mu\mu} < 1500$ GeV	12	20.3 fb <sup>-1</sup>	ATLAS 8 TeV [47] Table 9
$e^+e^-$	$80 < m_{ee} < 6000$ GeV	9	36.1 fb <sup>-1</sup>	ATLAS 13 TeV [48] Table 6
$\mu^+\mu^-$	$80 < m_{\mu\mu} < 6000$ GeV	9	36.1 fb <sup>-1</sup>	ATLAS 13 TeV [48] Table 7
$e^+e^-$	$120 < m_{ee} < 1800_+$ GeV	6	36. fb <sup>-1</sup>	CMS 13 TeV [49] Table 2
$\mu^+\mu^-$	$120 < m_{\mu\mu} < 1800_+$ GeV	6	36. fb <sup>-1</sup>	CMS 13 TeV [49] Table 3

As for the monojet analysis, we use the CMS results [40] at 13 TeV with an integrated luminosity of 35.9 fb<sup>-1</sup>. The CMS analysis was done as a counting experiment in 22 independent signal regions satisfying  $E_T^{\text{miss}} > 250$  GeV,  $p_T^{\text{jet}} > 100$  GeV and  $|\eta_j| < 4.5$ . For each of the above experiments and channels, we extract from the experimental publications the observed event rates in each bin  $N_{\text{obs}}^i$ , the background expectations  $N_{\text{bkg}}^i$ , and the SM predictions  $N_{\text{SM}}^i$ , as well as the statistical and systematic errors.

In order to confront the leptoquark predictions with the available data, first we simulate the processes (2.2) and (2.3) using MADGRAPH5\_AMC@NLO [50] with the UFO files for our effective lagrangian generated with FEYNRULES [51, 52]. The 8 TeV Drell-Yan simulation was carried out in next-to-leading order QCD at the parton level while the 13 TeV dilepton analyses were done in leading order using PYTHIA [53] to perform the parton shower, while the fast detector simulation was carried out with DELPHES [54]. In the jet plus missing transverse momentum analysis we

---

<sup>1</sup> We merged the two last bins in Ref. [48] to ensure gaussianity. The last bin of Ref. [49] (denoted by 1800<sub>+</sub>) is for  $m_{ee}(m_{\mu\mu}) > 1800$  GeV.

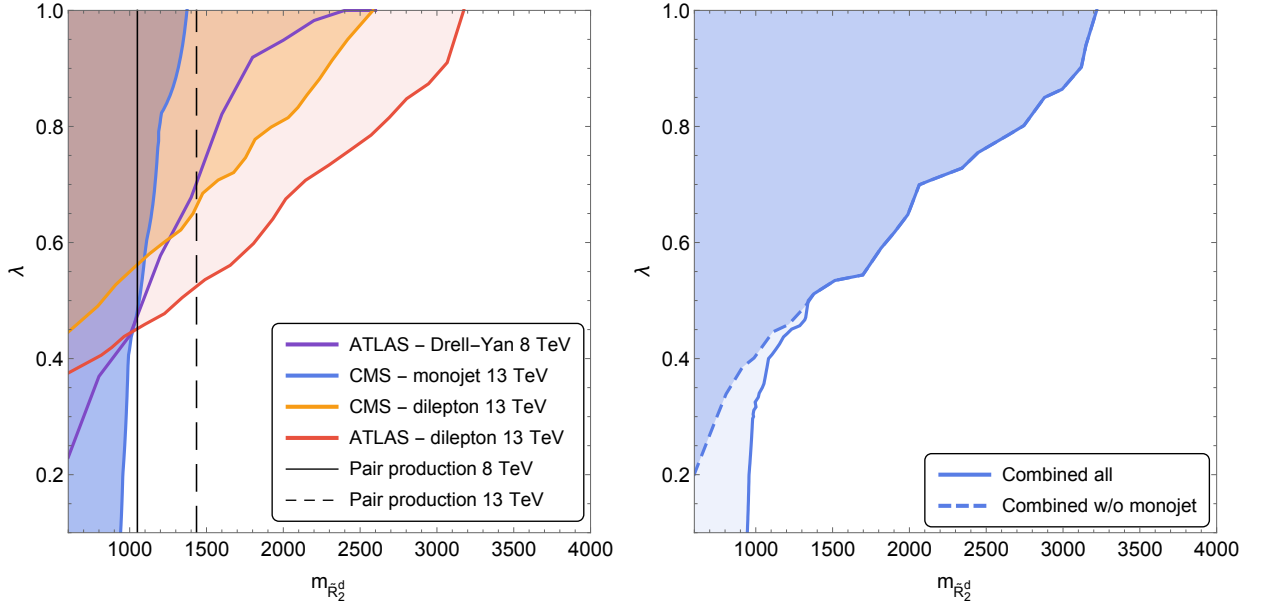


FIG. 1: Excluded regions at 95% CL for the  $\tilde{R}_2^d$  scenario. *Left*: limits from the ATLAS Drell-Yan search at 8 TeV (purple) [47], the CMS monojet search at 13 TeV (blue) [40], the CMS and ATLAS dilepton searches at 13 TeV (yellow and red, respectively) [48, 49], and the pair production experimental searches at 8 and 13 TeV (black solid and black dashed, respectively) [2, 28–30]. *Right*: combined limits including all searches (solid blue) and excluding only the monojet one (dashed blue).

merged the Monte Carlo simulations containing 0, 1 and 2 jets and performed the jet matching. In order to account for higher order corrections and additional detector effects we normalized bin by bin our dilepton simulations to the corresponding ones performed by the experimental collaborations. Then we apply these correction factors to our simulated distributions taking into account the leptoquark contributions.

In order to perform the statistical analysis we defined a  $\chi^2$  function for the dilepton analysis given by<sup>2</sup>

$$\chi_{\ell\ell}^2(m_R, \lambda) = \sum_i \frac{(N_{\text{sig}}^i(m_R, \lambda) + N_{\text{bkg}}^i - N_{\text{obs}}^i)^2}{N_{\text{obs}}^i + \sigma_{\text{bkg}}^{i2}}, \quad (2.4)$$

where  $N_{\text{sig}}$  are the signal events obtained for the different models using the corrections factors and  $\sigma_{\text{bkg}}^i$  are the uncertainty on the background obtained by the experiments. Here  $m_R$  ( $\lambda$ ) stands for the leptoquark mass (Yukawa coupling). On the other hand, for the monojet searches we used a gaussian likelihood containing the correlation between the different bins obtained in Ref. [40]

$$\chi_{\text{monojet}}^2(m_R, \lambda) = \sum_{i,j} (N_{\text{sig}}^i(m_R, \lambda) + N_{\text{bkg}}^i - N_{\text{obs}}^i)(\sigma^2)_{ij}^{-1} (N_{\text{sig}}^j(m_R, \lambda) + N_{\text{bkg}}^j - N_{\text{obs}}^j), \quad (2.5)$$

where  $\sigma_i^2 = \sigma_i \rho_{ij} \sigma_j$  and  $\rho$  is the correlation matrix. Finally, the combined results are obtained with the following  $\chi^2$ :

$$\chi_{\text{combined}}^2(m_R, \lambda) = \sum_i \chi_i^2(m_R, \lambda), \quad (2.6)$$

where  $i$  runs over the different searches (Drell-Yan, dilepton and monojet).

<sup>2</sup> In the Drell-Yan analysis, we estimated the effect of the systematic uncertainties by means of a simplified treatment in terms of two pulls [55, 56].

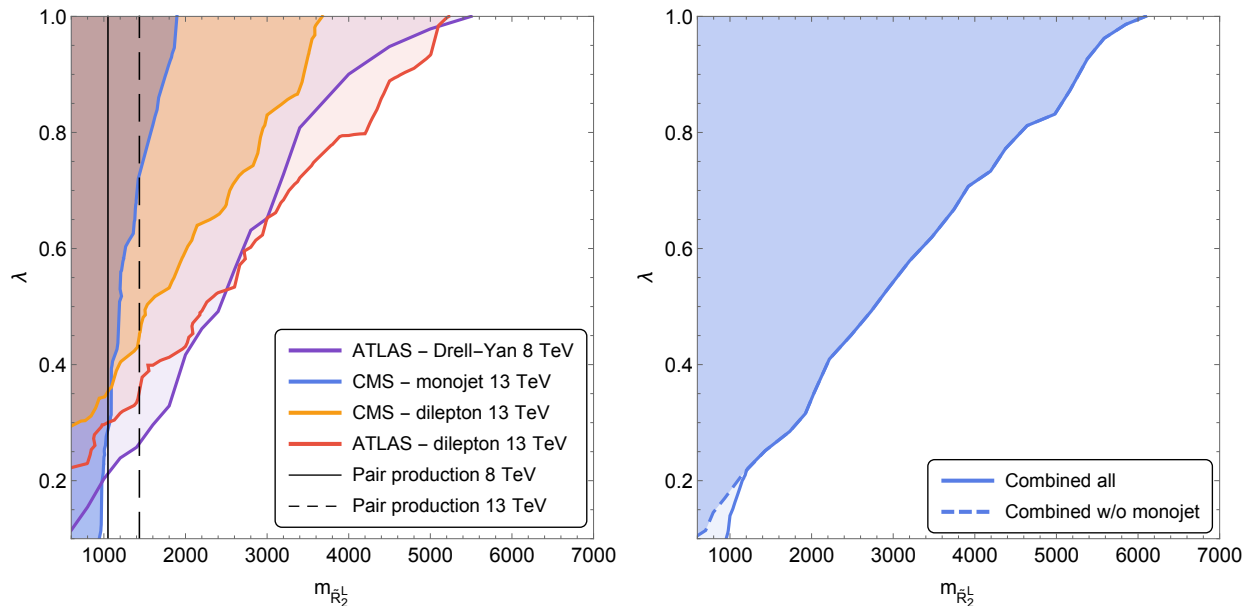


FIG. 2: Excluded regions at 95% CL for the  $R_2^L$  scenario. *Left*: limits from the ATLAS Drell-Yan search at 8 TeV (purple) [47], the CMS monojet search at 13 TeV (blue) [40], the CMS and ATLAS dilepton searches at 13 TeV (yellow and red, respectively) [48, 49], and the pair production experimental searches at 8 and 13 TeV (black solid and black dashed, respectively) [2, 28–30]. *Right*: combined limits of the Drell-Yan and dilepton searches. *Right*: combined limits including all searches (solid blue) and excluding only the monojet one (dashed blue).

### III. RESULTS

We start our analyses considering the first-generation scenarios. In Figure 1 we present the results of our analyses for the  $\tilde{R}_2^d$  case. The left panel of this figure depicts the excluded regions at 95% CL for each of the four data sets described in the previous section. The shaded purple region on the left of the curve is excluded by the Drell-Yan analysis of the ATLAS 8 TeV search. The blue area is excluded by the CMS monojet analysis at 13 TeV, while the CMS and ATLAS dilepton analysis of 13 TeV data exclude the yellow and red regions, respectively. Finally, for the sake of comparison, the solid and dashed black lines show the exclusion from the pair production experimental searches at 8 and 13 TeV, respectively. As we can see, the most stringent limits from masses above 1 TeV originates from the ATLAS data on the search of new resonances decaying into  $e^+e^-$  pair [48]. On the other hand, in the low mass region ( $\simeq 1$  TeV) the monojet data leads to stronger limits on the leptoquark  $\tilde{R}_2$  than the dilepton analysis.

When we combine the three datasets on dileptons, as shown by the dashed blue curve in the right panel of Fig. 1, we see that the bounds are basically due to the ATLAS 13 TeV data on dileptons, except for masses smaller than 700 GeV where the stronger limits come from the 8 TeV Drell-Yan analysis. Furthermore, the inclusion of the monojet data in the combined  $\chi^2$  strengthen the limits for low leptoquark masses, as shown by the solid blue curve. It is important to keep in mind that the combination of dilepton and monojet constraints is only possible because we assumed that the leptoquarks belonging to the multiplet  $\tilde{R}_2$  are degenerate.

We expect stronger constraints on the  $R_2^L$  scenario than on the  $\tilde{R}_2^d$  one since the former couples to up quarks while the latter to down quarks. This indeed happens as shown in Figure 2. In the left panel the purple, blue, yellow and red shaded regions correspond respectively to 95% CL limits from 8 TeV ATLAS Drell-Yan, 13 TeV CMS monojet, 13 TeV CMS dilepton and 13 TeV ATLAS dilepton searches. Moreover, the black solid and dashed lines denotes the 95% CL experimental constraints from pair production at 8 and 13 TeV.

We learn from the left panel of this figure that for masses below 1 TeV the monojet data give rise to the tighter bounds than the dilepton study. On the other hand, for larger masses the ATLAS dilepton data at 13 TeV and the

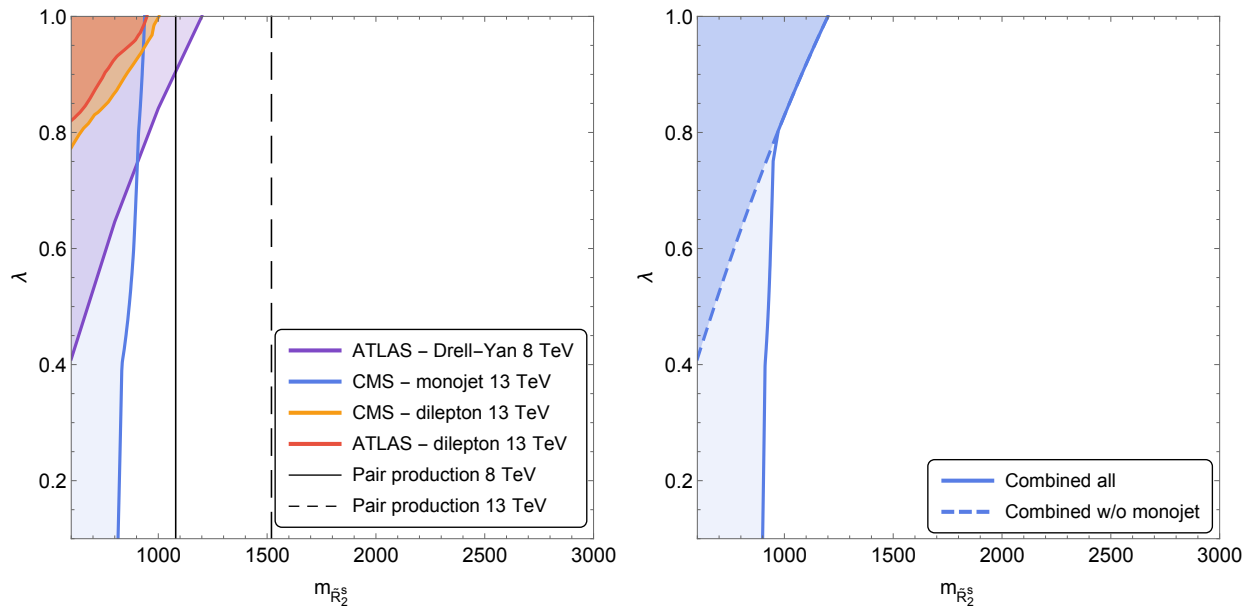


FIG. 3: Excluded regions at 95% CL for the  $\tilde{R}_2^s$  scenario. *Left*: limits from the ATLAS Drell-Yan search at 8 TeV (purple) [47], the CMS monojet search at 13 TeV (blue) [40], the CMS and ATLAS dilepton searches at 13 TeV (yellow and red, respectively) [48, 49], and the pair production experimental searches at 8 and 13 TeV (black solid and black dashed, respectively) [2, 28–30]. *Right*: combined limits including all searches (solid blue) and excluding only the monojet one (dashed blue).

ATLAS 8 TeV Drell-Yan data lead to similar constraints. Despite the lower integrated luminosity and energy the 8 TeV Drell-Yan limits are similar to the 13 TeV ones since the Drell-Yan cuts and presentation of the data are more suitable for the present study.

The right panel of Fig. 2 contains the limits obtained combining the dilepton datasets only (dashed blue curve) as well as limits including the monojet one (solid blue line). In this scenario, the combined dilepton bounds are tighter than the separate limits. Moreover, the inclusion of the monojet data give rise to stronger limits for masses below 1 TeV.

The scenario  $\tilde{R}_2^s$  provides the strongest limits on second generation leptoquarks due to its coupling to strange quarks. We display in Figure 3 the results for this scenario, with the same color coding of the previous Figures. The most stringent dilepton limits come from the 8 TeV Drell-Yan analysis with the ATLAS and CMS 13 TeV data leading to similar weaker constraints; see the left panel of this figure. Moreover, the impact of the monojet is similar to the ones of the other cases: the monojet data leads to the best bounds for small to moderate Yukawa couplings, due to the small dilepton cross section at small couplings. This fact can be clearly seen on the left panel of this figures that depicts the results combining only the dilepton searches (blue dashed curve) or including the monojet dataset (solid blue line). The left panel shows also that, for this scenario, the pair production searches still give the strongest constraints.

#### IV. DISCUSSION

The indirect leptoquark signal in the Drell-Yan process is complementary to the pair production searches since it is able to probe higher leptoquark masses. On the other hand, the indirect analysis requires the introduction of the unknown leptoquark Yukawa coupling. To illustrate this point let us focus on the 8 TeV data and first-generation leptoquarks. From the left panel of Fig. 1 we see that the analysis of indirect effects on the Drell-Yan production expands the excluded region by the pair production search for Yukawa couplings  $\lambda \gtrsim 0.5$ . In fact, the 8 TeV indirect

limits are still more stringent than the direct searches at 13 TeV for Yukawa couplings  $\lambda \gtrsim 0.7$ . Moreover, when we consider all available 13 TeV data, the indirect limits are stronger than the pair production ones for Yukawa couplings  $\lambda \gtrsim 0.5$  and extend the exclusion region to leptoquark masses of the order of 3.5 TeV if the leptoquark Yukawa coupling is  $\lambda \sim 1$ .

The importance of the indirect effects is even more dramatic when we consider the  $R_2^L$  scenario where the scalar leptoquark couples to up quarks. Indeed, Fig. 2 shows that the 8 TeV Drell-Yan limits are more stringent than the presently available 13 TeV direct search limits for Yukawa couplings  $\lambda \gtrsim 0.25$ . In addition, the combined 8 and 13 TeV dilepton data allow the exclusion of leptoquarks with mass smaller than 7 TeV provided the Yukawa coupling is  $\lambda \sim 1$ . In the case of second generation leptoquarks, scenario  $\tilde{R}_2^s$ , the impact of the leptoquarks in the dilepton invariant mass spectrum is much smaller due to its coupling to strange quarks. Therefore, the indirect limits turn out to be milder than the pair production ones that proceed through strong interactions; see Fig. 3.

Our monojet analyses lead to limits that complement the dilepton studies at low leptoquark masses (smaller than 1 TeV). For large Yukawa coupling, *e.g.*  $\lambda \sim 1$ , the monojet analysis exclude leptoquarks with masses up to 2 TeV (950 GeV) for first- (second-) generation leptoquarks. Notwithstanding, for this region of Yukawa couplings the indirect dilepton process leads to much stronger constraints. Furthermore, our results indicate that the monojet channel and the single production of leptoquarks decaying into a charged lepton and a jet [33] have similar capability to search for these particles. On the other hand, for second generation leptoquarks the monojet search is not competitive with respect to the dilepton analysis.

Confronting the monojet bounds on first-generation leptoquarks with ones originating from the ongoing studies of the  $\ell^+\ell^-jj$  and  $\ell^\pm\nu jj$  topologies [2], we learn that the monojet search leads to tighter bounds than these pair production searches only for Yukawa couplings  $\lambda \gtrsim 0.7$  in the  $\tilde{R}_2^L$  scenario. Furthermore, our results show that the monojet channel extends considerably the exclusion limits originating from leptoquark pair production followed by their decay into a jet and a neutrino, *i.e.* the  $jjE_T^{\text{miss}}$  channel [41].

Finally, we can abandon the hypothesis of degeneracy of leptoquarks belonging to the same multiplet if we consider separately the dilepton and monojet constraints. In this case, we have to examine the couplings of each component of the leptoquark multiplets:

1. the dilepton bounds on  $\tilde{R}_2^d$  applies to all leptoquarks that couples to electrons and down quarks, that is,  $\tilde{S}_1$ , the components 1 and 2 of  $\tilde{S}_3$ , the down component of  $R_2$  with right-handed couplings, and the up component of  $\tilde{R}_2^d$  (of course);
2. the dilepton constraints on  $R_2$  are the same for  $S_1$ , the third component of  $\vec{S}_3$  and the up (down) component of  $R_2$  with left-handed (right-handed) coupling;
3. the monojet analyses labeled  $\tilde{R}_2^d$  is the same for  $S_1$ , the third component of  $\vec{S}_3$  and the down component of  $\tilde{R}_2^d$ . Our  $R_2^L$  monojet study is valid for the components 1 and 2 of  $\vec{S}_3$  and the down component of  $R_2$  with left-handed couplings.

## V. CONCLUSIONS

In this work, we have considered collider constraints on first- and second-generation leptoquarks. In particular, we studied the  $\tilde{R}_2$  scalar leptoquark model with couplings only to the right-handed down (strange) quark and the first- (second-) generation lepton doublet, and the  $R_2$  scalar leptoquark model with couplings only to the right-handed up quark and the first generation left-handed lepton doublet. Stringent experimental bounds on leptoquarks come from their pair production followed by their prompt decays. This production mechanism is independent of the leptoquarks Yukawa coupling. For large leptoquark Yukawa couplings, on the other hand, single production becomes important. This is especially relevant for couplings with the first generation quarks because of their large parton distribution functions.

Our results show the importance of the search for leptoquark effects in the Drell-Yan process since it allows to extend considerably the reach in leptoquark mass for moderate to large leptoquark Yukawa couplings. For example, the scalar  $\tilde{R}_2$  ( $R_2$ ) leptoquark model with couplings to the first-generation quark is excluded up to  $\sim 3.2$  ( $\sim 5.6$ ) TeV for  $\lambda \sim 1$ , overcoming the pair production limits  $\lesssim 1.5$  TeV. In addition, we showed that the monojet channel is a viable alternative to further probe leptoquarks. Moreover, should a signal arise at the LHC, these kind of processes would give more information on the leptoquark properties, given their dependence on the leptoquark mass and Yukawa coupling.

Finally, we discussed how to interpret the results obtained in this work if we abandon the hypothesis of degeneracy of the leptoquarks belonging to the same  $SU(2)$  multiplet and the possible connection to constraints on the singlet ( $S_1$ ) or each component of the triplet ( $S_3$ ) scalar leptoquark models.

### Acknowledgments

This work is supported in part by Conselho Nacional de Desenvolvimento Científico e Tecnológico (CNPq) and by Fundação de Amparo à Pesquisa do Estado de São Paulo (FAPESP) grant 2012/10095-7. A. Alves thanks Conselho Nacional de Desenvolvimento Científico (CNPq) for its financial support, grant 307265/2017-0. R.R. Moreira was supported by FAPESP process no. 2013/26511-1. GGdC has been supported by the FAPESP process no. 2016/17041-0 and by the National Science Centre, Poland, under research grant no. 2017/26/D/ST2/00225. GGdC would like to thank FAPESP grant 2016/01343-7 for funding his visit to ICTP-SAIFR during November 2018 where part of this work was done.

- 
- [1] M. Aaboud et al. (ATLAS), New J. Phys. **18**, 093016 (2016), 1605.06035.
  - [2] A. M. Sirunyan et al. (CMS), Submitted to: Phys. Rev. (2018), 1811.01197.
  - [3] J. C. Pati and A. Salam, Phys. Rev. **D8**, 1240 (1973).
  - [4] J. C. Pati and A. Salam, Phys. Rev. **D10**, 275 (1974), [Erratum: Phys. Rev.D11,703(1975)].
  - [5] H. Georgi and S. L. Glashow, Phys. Rev. Lett. **32**, 438 (1974).
  - [6] B. Schrempp and F. Schrempp, Phys. Lett. **153B**, 101 (1985).
  - [7] R. Barbier et al., Phys. Rept. **420**, 1 (2005), hep-ph/0406039.
  - [8] O. U. Shanker, Nucl. Phys. **B206**, 253 (1982).
  - [9] I. Dorsner, S. Fajfer, A. Greljo, J. F. Kamenik, and N. Kosnik, Phys. Rept. **641**, 1 (2016), 1603.04993.
  - [10] J. K. Mizukoshi, O. J. P. Eboli, and M. C. Gonzalez-Garcia, Nucl. Phys. **B443**, 20 (1995), hep-ph/9411392.
  - [11] G. Bhattacharyya, J. R. Ellis, and K. Sridhar, Phys. Lett. **B336**, 100 (1994), [Erratum: Phys. Lett.B338,522(1994)], hep-ph/9406354.
  - [12] J. P. Lees et al. (BaBar), Phys. Rev. Lett. **109**, 101802 (2012), 1205.5442.
  - [13] R. Aaij et al. (LHCb), Phys. Rev. Lett. **115**, 111803 (2015), [Erratum: Phys. Rev. Lett.115,no.15,159901(2015)], 1506.08614.
  - [14] M. Huschle et al. (Belle), Phys. Rev. **D92**, 072014 (2015), 1507.03233.
  - [15] Y. Sato et al. (Belle), Phys. Rev. **D94**, 072007 (2016), 1607.07923.
  - [16] Y. Amhis et al. (HFLAV), Eur. Phys. J. **C77**, 895 (2017), 1612.07233.
  - [17] R. Aaij et al. (LHCb), Phys. Rev. Lett. **111**, 191801 (2013), 1308.1707.
  - [18] R. Aaij et al. (LHCb), JHEP **02**, 104 (2016), 1512.04442.
  - [19] M. Ciuchini, M. Fedele, E. Franco, S. Mishima, A. Paul, L. Silvestrini, and M. Valli, JHEP **06**, 116 (2016), 1512.07157.
  - [20] R. Aaij et al. (LHCb), Phys. Rev. Lett. **113**, 151601 (2014), 1406.6482.
  - [21] R. Aaij et al. (LHCb), JHEP **08**, 055 (2017), 1705.05802.
  - [22] I. Dörner, S. Fajfer, N. Konik, and I. Niandi, JHEP **11**, 084 (2013), 1306.6493.
  - [23] Y. Sakaki, M. Tanaka, A. Tayduganov, and R. Watanabe, Phys. Rev. **D88**, 094012 (2013), 1309.0301.
  - [24] M. Bauer and M. Neubert, Phys. Rev. Lett. **116**, 141802 (2016), 1511.01900.
  - [25] R. Barbieri, G. Isidori, A. Pattori, and F. Senia, Eur. Phys. J. **C76**, 67 (2016), 1512.01560.



- [26] D. Becirevic, N. Kosnik, O. Sumensari, and R. Zukanovich Funchal, JHEP **11**, 035 (2016), 1608.07583.
- [27] J. L. Hewett and S. Pakvasa, Phys. Rev. **D37**, 3165 (1988).
- [28] G. Aad et al. (ATLAS), Eur. Phys. J. **C76**, 5 (2016), 1508.04735.
- [29] V. Khachatryan et al. (CMS), Phys. Rev. **D93**, 032004 (2016), 1509.03744.
- [30] A. M. Sirunyan et al. (CMS), Submitted to: Phys. Rev. (2018), 1808.05082.
- [31] O. J. P. Eboli and A. V. Olinto, Phys. Rev. **D38**, 3461 (1988).
- [32] M. Schmaltz and Y.-M. Zhong (2018), 1810.10017.
- [33] V. Khachatryan et al. (CMS), Phys. Rev. **D93**, 032005 (2016), [Erratum: Phys. Rev.D95,no.3,039906(2017)], 1509.03750.
- [34] B. Allanach, A. Alves, F. S. Queiroz, K. Sinha, and A. Strumia, Phys. Rev. **D92**, 055023 (2015), 1501.03494.
- [35] T. Lin, E. W. Kolb, and L.-T. Wang, Phys. Rev. **D88**, 063510 (2013), 1303.6638.
- [36] V. Khachatryan et al. (CMS), CMS-PAS-B2G-15-007 (2016).
- [37] G. Aad et al. (ATLAS), Eur. Phys. J. **C75**, 92 (2015), 1410.4031.
- [38] A. M. Sirunyan et al. (CMS), JHEP **06**, 027 (2018), 1801.08427.
- [39] A. M. Sirunyan et al. (CMS), Submitted to: Phys. Rev. Lett. (2018), 1807.06522.
- [40] V. Khachatryan et al. (CMS), CMS-PAS-EXO-16-048 (2017).
- [41] A. M. Sirunyan et al. (CMS), Phys. Rev. **D98**, 032005 (2018), 1805.10228.
- [42] W. Buchmuller, R. Ruckl, and D. Wyler, Phys. Lett. **B191**, 442 (1987), [Erratum: Phys. Lett.B448,320(1999)].
- [43] W. Buchmuller and D. Wyler, Phys. Lett. **B177**, 377 (1986).
- [44] S. Davidson, D. C. Bailey, and B. A. Campbell, Z. Phys. **C61**, 613 (1994), hep-ph/9309310.
- [45] M. Carpentier and S. Davidson, Eur. Phys. J. **C70**, 1071 (2010), 1008.0280.
- [46] M. Leurer, Phys. Rev. **D49**, 333 (1994), hep-ph/9309266.
- [47] G. Aad et al. (ATLAS), JHEP **08**, 009 (2016), 1606.01736.
- [48] M. Aaboud et al. (ATLAS), JHEP **10**, 182 (2017), 1707.02424.
- [49] A. M. Sirunyan et al. (CMS), JHEP **06**, 120 (2018), 1803.06292.
- [50] J. Alwall, R. Frederix, S. Frixione, V. Hirschi, F. Maltoni, O. Mattelaer, H. S. Shao, T. Stelzer, P. Torrielli, and M. Zaro, JHEP **07**, 079 (2014), 1405.0301.
- [51] N. D. Christensen and C. Duhr, Comput. Phys. Commun. **180**, 1614 (2009), 0806.4194.
- [52] A. Alloul, N. D. Christensen, C. Degrande, C. Duhr, and B. Fuks, Comput. Phys. Commun. **185**, 2250 (2014), 1310.1921.
- [53] T. Sjostrand, S. Mrenna, and P. Z. Skands, JHEP **05**, 026 (2006), hep-ph/0603175.
- [54] J. de Favereau, C. Delaere, P. Demin, A. Giammanco, V. Lemaitre, A. Mertens, and M. Selvaggi (DELPHES 3), JHEP **02**, 057 (2014), 1307.6346.
- [55] G. L. Fogli, E. Lisi, A. Marrone, D. Montanino, and A. Palazzo, Phys. Rev. **D66**, 053010 (2002), hep-ph/0206162.
- [56] M. C. Gonzalez-Garcia and M. Maltoni, Phys. Rept. **460**, 1 (2008), 0704.1800.